

NOTICE

This report was prepared as an account of work sponsored by the United States Government. Neither the United States nor the United States Atomic Energy Commission, nor any of their employees, nor any of their contractors, subcontractors, or their employees, makes any warranty, express or implied, or assumes any legal liability or responsibility for the accuracy, completeness or usefulness of any information, apparatus, product or process disclosed, or represents that its use would not infringe privately owned rights.

COO #3344-9

33828

OK  
T

ANNUAL REPORT

and

PROPOSAL FOR RENEWAL OF CONTRACT NO. AT(11-1)-3344

Basic Research in Crystalline and Noncrystalline Ceramic Systems

THIS DOCUMENT CONFIRMED AS  
UNCLASSIFIED  
DIVISION OF CLASSIFICATION  
BY IL Cucchiaro/pah  
DATE 7/23/73

Principal Investigator  
(On Sabbatical in 1971-72)

W. D. Kingery, Professor of Ceramics

Principal Investigator

R. L. Coble  
R. L. Coble, Professor of Ceramics

Head of Department

T. B. King, Head  
Department of Metallurgy and  
Materials Science

Division of Sponsored Research

G. H. Dummer, Director

Massachusetts Institute of Technology  
Cambridge, Massachusetts 02139

**MASTER**

This report was prepared as an account of work sponsored by the United States Government. Neither the United States nor the United States Atomic Energy Commission, nor any of their employees, nor any of their contractors, subcontractors, or their employees, makes any warranty, express or implied, or assumes any legal liability or responsibility for the accuracy, completeness or usefulness of any information, apparatus, products or process disclosed, or represents that its use would not infringe privately owned rights. \$1.701

## **DISCLAIMER**

**This report was prepared as an account of work sponsored by an agency of the United States Government. Neither the United States Government nor any agency Thereof, nor any of their employees, makes any warranty, express or implied, or assumes any legal liability or responsibility for the accuracy, completeness, or usefulness of any information, apparatus, product, or process disclosed, or represents that its use would not infringe privately owned rights. Reference herein to any specific commercial product, process, or service by trade name, trademark, manufacturer, or otherwise does not necessarily constitute or imply its endorsement, recommendation, or favoring by the United States Government or any agency thereof. The views and opinions of authors expressed herein do not necessarily state or reflect those of the United States Government or any agency thereof.**

## **DISCLAIMER**

**Portions of this document may be illegible in electronic image products. Images are produced from the best available original document.**

## I. INTRODUCTION

The basic research program in ceramics sponsored by the U. S. Atomic Energy Commission supports the majority of the ceramic research effort and graduate student training in ceramics at M.I.T. Various research subjects have been investigated in the past including heat conduction, surface characteristics, diffusion in oxides, high-temperature kinetic processes, microstructure development, effects of microstructure on properties, the structure and properties of noncrystalline ceramics, dissolution kinetics, materials preparation, and solid-vapor reactions. The current program is described in Section II, which follows.

The research program this past year has been supervised by Professor R. L. Coble; Professors Wuensch and Bowen have also participated. The experimental work is mostly performed by graduate students working towards advanced degrees, along with technicians and research staff. For the current research described in the following section, supervising staff members and students are identified for each individual project. All work has been planned with and approved by Professor Coble.

During this year staff members associated with this program have remained familiar with other Atomic Energy Commission programs in ceramics by visiting or receiving visits from personnel at the Argonne National Laboratory, Battelle-Northwest, and Oak Ridge National Laboratory. We have also visited nuclear materials research laboratories at Grenoble in France, and Boris Kidric Institute in Belgrade, Yugoslavia.

## II. PRESENT STATUS

At the present time projections indicate the  $UO_2$  and other ceramics for nuclear fuel applications will be a critical factor in nuclear power development and also become a major product of the ceramic industry. Thus,

development of new understanding of phenomena in the field of crystalline and noncrystalline ceramics outside of the traditional silicate based clay-glass-cement sector seems certain to be applicable to A.E.C. responsibilities. These considerations have led us to continue our concentration on fluorite-structure materials and on nonstoichiometry, solid solutions and grain boundary phenomena in oxide systems.

The current research program in ceramics at M.I.T. can be broadly described as including: (1) research on kinetics of phase changes, diffusion, and the development of microstructure in ceramics, (2) relationship of properties to composition, crystal structure, and microstructure, (3) research on the structure and properties of thin films and noncrystalline solids, and (4) materials synthesis and preparation. Each of these areas of research is described in detail in the report.

SECTION ONE

- 1.0 Defects, Diffusion Kinetics of Phase Changes and Microstructure Development
- 1.1 R. L. Coble and K. Kitazawa: Defect Diffusion Coefficient in Polycrystal Alumina
- 1.2 R. L. Coble and W. L. Robbins: Characterization of Defects and Diffusivities in Doped Single Crystal Aluminum Oxide
- 1.3 B. J. Wuensch and D. J. Reed: Mass Transport in Crystals
- 1.4 B. J. Wuensch and K. S. Kim: Mass Transport in Crystals
- 1.5 R. L. Coble and U. Chowdry: Survey of Diffusion Studies on the Transition Metal Monoxides
- 1.6 R. L. Coble and J. Neve: Sintering of  $\text{Cr}_2\text{O}_3$
- 1.7 R. L. Coble and L. Radonjic: Characterization of the Morphological Evolution in a Two-Phase Isotropic System
- 1.8 R. L. Coble and C. F. Yen: Spheroidization of Tubular Voids in Alumina Crystals at High Temperatures
- 1.9 R. L. Coble, S. C. Samanta and C. F. Yen: Kinetics for the Intermediate Stage Sintering of Silver
- 1.10 R. L. Coble: Some Particle Size Distribution Effects in Sintering
- 1.11 H. K. Bowen and D. D. Marchant: Thermal Gradient Studies
- 1.12 H. K. Bowen and D. D. Marchant: Thermal Gradient Studies in  $(\text{U,Ce})\text{O}_2$  Compositions

SECTION TWO

- 2.0 Material Preparation; High Purity Single Crystal Growth
- 2.1 R. L. Coble, H. K. Bowen, R. N. Singh and D. D. Marchant: CVD  
Growth of  $UO_{2+x}$  Single Crystals
- 2.2 W. D. Kingery, H. K. Bowen and J. R. Booth: Growth and Properties  
of CVD Grown Single Crystals of MgO and MgO- $Al_2O_3$
- 2.3 W. D. Kingery, H. K. Bowen and L. P. Ferrao: Growth of Single  
Crystals of  $ZrO_2-Y_2O_3$  Solid Solutions by Chemical Vapor  
Deposition in a Dynamic System
- 2.4 W. D. Kingery and C. C. Seaton: Polycrystalline Growth of  $Y_2O_3-ZrO_2$   
Solid Solutions by Chemical Transport
- 2.5 H. K. Bowen: Chemical Vapor Deposition of ZnS on GaP
- 2.6 R. L. Coble and R. L. Gentilman: Growth of Single Crystal Epitaxial  
Films of  $Y_3Fe_5O_{12}$  by Chemical Vapor Deposition
- 2.7 H. K. Bowen, W. D. Kingery and M. Kinoshita: Chemical Vapor Transport  
and Phase Studies in  $Co_xNi_{1-x}O$
- 2.8 R. L. Coble and W. M. Smith: Co-Doping in Ultra-High Purity Materials

SECTION THREE

- 3.0 Electrical Properties
- 3.1 W. D. Kingery and J. Sauvage: Electrical Behavior of Amorphous Silicon as Revealed by Tunneling and Related Experiments
- 3.2 H. K. Bowen; L. P. C. Ferrao, D. D. Marchant, R. N. Singh, K. Uematsu: Effects of Thermal-Neutron Irradiation on Amorphous-Silicon Film
- 3.3 R. L. Coble and K. Kitazawa: Electric Conduction Mechanism in Alumina
- 3.4 R. L. Coble and K. Kitazawa: Stabilized Zirconia as an Oxygen Permeation Measurement Detector



SECTION FOUR

- 4.0 Crystal Structure and Properties
- 4.1 B. J. Wuensch and H. T. Anderson: Nonstoichiometric Oxides with the Fluorite Structure Types
- 4.2 R. L. Coble and C. V. Hari Rao: Strain Centers in Sapphire
- 4.3 R. L. Coble, H. K. Bowen and J. L. Caslavsky: X-ray Topography of Oxides
- 4.4 R. L. Coble and R. N. Singh: Dislocation Behavior in Pure and Doped (Fe) Single Crystals of MgO
- 4.5 R. L. Coble and R. M. Cannon: Grain Boundary Sliding in Oxide Ceramics
- 4.6 W. D. Kingery, H. K. Bowen and C. A. Goodwin: Optical and Electrical Properties of Single Crystal  $Fe_xO$ -MnO Solid Solutions
- 4.7 H. K. Bowen and B. H. Auker: Low Temperature Conductivity and Reflectivity of CVD Wustite

## 1.0 Defects, Diffusion, Kinetics of Phase Changes and Microstructure Development

### 1.1 Defect Diffusion Coefficient in Polycrystal Alumina (Professor R. L. Coble; K. Kitazawa)

*see p. 51, bottom*

In order to better understand the mechanism of grain boundary enhanced diffusion, defect diffusion coefficients in polycrystal alumina were measured by electrical conductivity following a step-wise change of the atmosphere. The observed time relaxation curve was well explained by a model assuming that: 1) polycrystal alumina is dominantly an electronic conductor; 2) the electronic defects are generated to compensate the charge of excess atomic defects; and 3) the atomic defects are generated or annihilated by the oxygen incorporation reaction which is rate controlled by the diffusion process of the defects. Defect diffusion coefficient was obtained for polycrystalline samples with different grain size and with different impurity content. The results may be represented by:

a) Hot-pressed non-doped sample (GS = 4 $\mu$ )

$$D_d = 5.3 \exp\left(-\frac{47.1 \text{ kcal}}{RT}\right) \text{ cm}^2/\text{sec}; \quad 1100-1330^\circ\text{C}$$

b) Hot-pressed non-doped sample (GS = 15 $\mu$ )

$$D_d = 1.7 \exp\left(-\frac{47 \text{ kcal}}{RT}\right) \text{ cm}^2/\text{sec}; \quad 1197-1305^\circ\text{C}$$

c) MgO-doped sample (LUCALOX) (GS = 30 $\mu$ )

$$D_d = 2.0 \times 10^{-2} \exp\left(-\frac{18.7 \text{ kcal}}{RT}\right) \text{ cm}^2/\text{sec}; \quad 1100-1350^\circ\text{C}$$

The results obtained showed the following characters:

- 1) The  $D_d$  in polycrystal alumina is a few orders of magnitude larger than that in single crystal;
- 2) The  $D_d$  is increased with decreasing grain size;
- 3) The  $D_d$  is enhanced by the presence of Mg impurity.

Comparing the present data with the other available data, the defect concentration in polycrystal alumina was roughly estimated. Although the defect is not identified yet, the following may be concluded from the present study: the defect of aluminum or oxygen ion, whichever diffuses faster, is itself enhanced in its diffusion on grain boundaries and is also enhanced by some impurities. This indicates that the possible mechanism of grain boundary diffusion is not only related to possible increased defect concentrations near boundaries, but also to enhanced motion of the defects on the boundaries.

## 1.2 Characterization of Defects and Diffusivities in Doped Single Crystal Aluminum Oxide

(Professor R. L. Coble; W. L. Robbins)

Investigation of the defect structure and diffusivities in doped and undoped single crystal aluminum oxide was undertaken.

Diffusivities and mobilities in titanium doped single crystal aluminum oxide were determined by the observation of a color boundary migration. Titanium doped single crystals of aluminum oxide are pink in a reduced condition. Upon oxidation, they become clear with the clearing taking place by a color boundary migration. When oxidation of previously reduced crystals takes place in the presence of a d-c field, color boundary migration parallel to the field and away from the anode is enhanced. The color boundary migration perpendicular to the d-c field allows determination of a diffusion coefficient, while that parallel allows determination of a mobility.

The results of this work indicate that aluminum oxide is a material in which both time and temperature processes as well as atmospheric effects must be considered. Factors effecting the color boundary migration were found to be reducing times and temperatures, oxidizing times and temperatures, background impurity content, and titanium concentration. Diffusion

models indicate that the color boundary migration is the result of at least two mobile species.

Lattice parameters and densities were determined for doped and undoped single crystals containing various background impurities. These crystals were investigated in both an oxidized (air annealed) and reduced (nitrogen annealed) condition. From the measured lattice parameters, densities were compared to the measured results with the best agreement being obtained when association of divalent and tetravalent impurities is assumed according to the following reaction:



In addition, the lattice parameter determinations indicate an expansion of the lattice, particularly in the c-direction resulting from the impurities and dopants present.

### 1.3 Mass Transport in Crystals

(Professor B. J. Wuensch; D. J. Reed)

The anisotropy of transport in ultra-high purity  $Al_2O_3$  is being studied. It is hoped to obtain tracer diffusion data at temperatures as close as possible to the melting point of the material in order to reveal a regime of intrinsic transport. Since isotopes suitable for conventional specimen preparation are not available for either Al or O, it is planned to analyze the samples by means of novel mass spectrometric methods. Work is proceeding on sample preparation to insure that the ultra-high purity of the crystals can be maintained. X

### 1.4 Mass Transport in Crystals

(Professor B. J. Wuensch; K. S. Kim)

Cation self-diffusion in single-crystal ZnO was measured as a function of temperature and crystallographic direction in an earlier

*see top  
p. 50*

portion of this study. These results indicated that diffusion is isotropic, within experimental error. The magnitude of the diffusion parameters observed, along with the lack of anisotropy, suggests that extrinsic diffusion via zinc vacancies had been observed, and not the migration of interstitial zinc in terms of which mass transport in this material had been previously interpreted.

Study of  $Zn^{65}$  diffusion in zinc oxide has been extended to include measurement of dislocation and grain-boundary diffusion rates. Low temperature (750°-1000°C) isotope gradients in single-crystals display a "tail" indicative of a contribution from a second mass transport mechanism. These portions of the gradients have been analyzed in terms of Suzuoka's exact theory to provide as dislocation pipe diffusion coefficients:

$$\text{along } \underline{a}: \delta D^{\circ}_a = 7 \cdot 10^{-8} \exp(-2.0 \pm 0.4 \text{ eV/KT})$$

$$\text{along } \underline{b}: \delta D^{\circ}_c = 8 \cdot 10^{-11} \exp(-1.5 \pm 0.3 \text{ eV/KT}).$$

In view of the scatter in the data the difference in rates along the two crystallographic directions may not be significant. Polycrystalline compacts of ZnO display cation self-diffusion rates which are more rapid than those of single-crystal specimens. Between 950° and 1100°C the grain-boundary diffusion coefficient has an activation energy of 1.0 to 1.5 eV. The enhancement of transport at grain boundaries has been shown to exhibit a strong dependence on annealing time. The effect is therefore extrinsic in nature and is probably linked to non-stoichiometry at the boundary. We have recently initiated a similar study of anisotropy in ultra-high purity  $Al_2O_3$ .

### 1.5 Survey of Diffusion Studies on the Transition Metal Monoxides

(Professor R. L. Coble; U. Chowdry)

A literature survey of all the 3d transition metal oxides is being conducted to determine a system in which the weight change kinetics are diffusion controlled. The aim is to be able to obtain a significant result for a defect diffusion coefficient. Using dense polycrystalline specimens of varying grain size, it is possible to determine if the defect diffusion coefficient is enhanced along the grain boundaries. In the case of FeO, MnO and VO, the kinetics have been reported to be controlled by a surface reaction in certain atmospheres and certain temperature ranges.

Since the bulk diffusion coefficient is high in the transition metal oxides, no significant studies of enhanced diffusion along the grain boundaries have been reported. There is no literature on diffusion studies at dislocations for these materials.

A report is presently being compiled of all the pertinent diffusion data available to date on these materials.

### 1.6 Sintering of Cr<sub>2</sub>O<sub>3</sub>

(Professor R. L. Coble; J. Neve)

The effect of atmosphere on stoichiometry and thus diffusion rates has been established in the sintering of a number of oxides. Recently, essentially theoretically dense Cr<sub>2</sub>O<sub>3</sub> was obtained under oxygen partial pressures near 10<sup>-12</sup> atmospheres. Prior to this study, the sintering of Cr<sub>2</sub>O<sub>3</sub> at much higher oxygen partial pressures had been investigated assuming evaporation-condensation and volume diffusion mechanisms. The validity of some of the conclusions from these past studies is questionable because of the inadequate data. A sintering study of Cr<sub>2</sub>O<sub>3</sub> at various

oxygen partial pressures is needed to determine both the mechanisms and rate controlling steps involved. Intermediate stage sintering models will be applied and possibly altered in interpreting data. X

### 1.7 Characterization of the Morphological Evolution in a Two-Phase Isotropic System

(Professor R. L. Coble; L. Radonjic)

In order to better understand the evolution of the microstructure, an isotropic two-phase system has been chosen for study. In a Vycor-type glass, after phase separation the phases are interconnected. Upon annealing, the interconnected structure may undergo morphological changes or simply coarsen depending on the specific form and the volume fractions of the phases.

Initial studies have been conducted on Vycor-type glass composition: 6% Na<sub>2</sub>O + 25.6% B<sub>2</sub>O<sub>3</sub> + 68.9% SiO<sub>2</sub>, which undergoes phase separation into multiply connected continuous network of the SiO<sub>2</sub>-rich and Na<sub>2</sub>O + B<sub>2</sub>O<sub>3</sub>-rich phase upon cooling through the immiscibility gap. After annealing in the temperature interval 560° to 710°C, the morphology has been examined by scanning electron microscopy.

For quantitative characterization of the interconnected structure, it is necessary to measure scale of structure  $\lambda$ , and the shape and degree of interconnectivity.

Measurement of the scale of the structure is now underway, using an optical Fourier transform method. Information about the apparent scale of structure observed in real space cannot be readily interpreted. It is necessary to perform a Fourier analysis of the texture in order to evaluate the (spinodal) wavelength (which is strictly defined only in reciprocal space). Using a laser as source of light and a micrograph as a diffraction grating the Fraunhofer diffraction spectrum is to be recorded,

no data

from which the wavelengths can be determined. Variations in wavelength with temperature, time histories, composition, or initial morphologies are the points of interest.

### 1.8 Spheroidization of Tubular Voids in Alumina Crystals at High Temperatures

(Professor R. L. Coble; C. F. Yen)

Cracks introduced into single crystal sapphires were observed, after annealing, to have broken up first into channels of cylindrical voids and ultimately into rows of spherical pores, with the thicker gap spacings in the original crack remaining open. Break-up of the cylindrical voids was studied upon subsequent annealing and found to conform to the models for surface diffusion controlled material transport. At the temperatures of measurement, the magnitudes of the surface diffusivities calculated are in good agreement with values reported earlier.

X  
see  
p. 50

### 1.9 Kinetics for the Intermediate Stage Sintering of Silver

(Professor R. L. Coble; S. C. Samanta and C. F. Yen)

Sintering of silver compacts of varying particle sizes was investigated in the intermediate stage of the process where densification rates are observed at known grain sizes in order to evaluate the kinetics models for the process when boundary diffusion is controlling. Grain growth kinetics are also measured and the kinetics are compared with those exhibited when sintering is controlled by lattice diffusion. Control by lattice diffusion was observed for silver at high temperatures and larger initial particle sizes.

X  
see  
p. 50

### 1.10 Some Particle Size Distribution Effects in Sintering

(Professor R. L. Coble)

Diffusion models for the initial stage sintering of spherical particles have been developed to cover distributions of particle sizes. Of various possible three-dimensional arrays of interest, only a linear



array of particles with the different sizes randomly distributed along it has been quantitatively handled. Analysis of that situation shows that number distributions rather than weight distributions must be considered to evaluate the particle pair interactions. Designation of a single particle size which will characterize the equivalent shrinkage of the distributed array of random particles shows that size is much smaller than the size which would designate the cut for 50 wt. pct. finer as is conventionally used. Also, the effective size is different for the lattice diffusion model than for the grain boundary diffusion controlled model. The results show that the rates for binary mixtures are intermediate between behaviors of the end member sizes, in accordance with earlier experimental findings.

? almost  
no data

### 1.11 Thermal Gradient Studies

(Professor H. K. Bowen; D. D. Marchant)

Some morphological and chemical properties of  $UO_{2+x}$  are being investigated after annealing in a thermal gradient. The current work is being done on polycrystalline sintered pellets. If quality single crystals can be obtained, some of these studies will be expanded to single crystals.

The basic procedure consists of imposing an axial thermal gradient along a row of sintered pellets. The pellets are then sliced and various properties are measured on each slice. Since each slice approximates an isothermal condition, various properties can be measured as a function of temperature and temperature gradient. Two other variables used are furnace atmosphere and time.

The morphological studies measure grain and pore size, shape and size distribution. The samples are also checked along the gradient to see if significant pore migration has occurred especially through the grains. The chemical measurement consists of determining the ratio of oxygen to uranium atoms (O/U) in the various slices. This ratio can change in a

thermal gradient. The change in this ratio depends on the various methods of migration of the oxygen and uranium ratios. The change in the ratio depends on several adjustable parameters like the furnace atmosphere, temperature, temperature gradient and experimental geometry, which are being varied to see their individual effects.

The thermal gradient measurements have been made in vacuum ( $10^{-3}$  torr) with a gradient from 1700°C to 1400°C over a 7 cm length of sintered pellets. The initial pellets were 92 to 95% theoretical density with an adjusted O/U ratio of 2.02, established by isothermally preannealing the samples in a controlled CO/CO<sub>2</sub> gas atmosphere. The thermal gradient anneals have been for times less than 24 hours. Grain growth has occurred above 1500°C. So far, no noticeable pore entrapment has occurred indicating only normal grain growth. The imposed gradients have not been high enough to find any pore migration. The O/U ratio remained unchanged with the method of measurement used. We attempted to determine the O/U ratio by measuring the lattice parameters with a Debye-Scherrer X-ray powder camera. This method is not precise enough since the changes in lattice parameters for this type of experiment are so small that they are within the limits of accuracy of the Debye-Scherrer technique.

Another method of determining the O/U ratio is by oxidizing the sample 950°C in air to U<sub>3</sub>O<sub>8</sub> and measuring the weight change, which requires a precise method of measuring weight changes. A Cahn Recording Microbalance is currently being used; the sensitivity of this unit is in micrograms which has allowed measurement of O/U ratios in the range of  $X = \pm 0.001$  for UO<sub>2+X</sub>.

### 1.12 Thermal Gradient Studies in (U,Ce)O<sub>2</sub> Compositions

(Professor H. K. Bowen; D. D. Marchant)

The understanding of fundamental migration phenomena in mixed oxide nuclear fuels is very important to the development of the mixed oxide reactor technology. Initial studies by various groups have hypothesized that diffusion migration becomes important at high temperatures, leading to hot end enrichment; which migration for plutonium greatly modifies reactor performance.

For diffusion migration a heat of transport  $Q^*$  can be kinetically defined as  $S = Q^*/RT^2$  where  $S$  = Soret coefficient. For a two component system of molar fractions,  $\lambda$  and  $1-\lambda$ ,  $S = \frac{1}{\lambda(1-\lambda)} \frac{d\lambda}{dT}$ . Therefore the heat of transport gives a parameter that indicates the amount of migration of components by a diffusion mechanism under steady state conditions.

The heat of transport appears to have a temperature dependence. This temperature dependence has not been determined for (U,Pu)O<sub>2</sub> due to the experimental problems at temperatures above 2400°C. Since (U,Ce)O<sub>2</sub> is a lower temperature system, the temperature dependence of the heat of transport can experimentally be measured. Two important applications can be made of this data. First, the temperature dependence can be related to (U,Pu)O<sub>2</sub>. Second, cerium is a common fission product and studying the migration can help in characterizing this and other fission product migration in the fuel matrix.

Initial studies have been made on fabrication of sintered pellets of high density. Uniform pellets have not been successfully fabricated by standard mixing and annealing techniques. Either freeze drying and/or solution precipitation techniques will be next tried.

To understand the effect of boundaries on the diffusional migration in (U,Ce)O<sub>2</sub> system, various thermal diffusion studies need to be made on single crystals. As part of our chemical vapor deposition single crystal

*no data*

studies, the growth of crystals of uniform  $(U,Ce)O_2$  will be attempted. This will require a special type of furnace design. The carrier gas will be chlorine. A dual injector will be designed to flow cerium chloride, uranium chloride and oxygen over the deposition area in controlled amounts. The composition of the resulting single crystals can be varied by adjusting the flows of the uranium and cerium gas species.

## 2.0 Material Preparation; High Purity Single Crystal Growth

### 2.1 CVD Growth of $UO_{2+x}$ Single Crystals

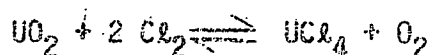
(Professor R. L. Coble; Professor H. K. Bowen; R. N. Singh and D. D. Marchant)

To elucidate whether other fluorite structure materials, namely  $UO_2$  and  $ThO_2$  show dislocation behavior similar to  $CaF_2$ , it was proposed to study the velocity of edge and screw dislocations as a function of stress, temperature and non-stoichiometry. However, because of the unavailability of good quality crystals it was decided to grow some crystals by chemical vapor deposition.

Preliminary feasibility studies were done by growing  $UO_2$  single crystals in a closed system using chlorine as transporting agent. The source material was  $UO_2$  powder and the substrate used was single crystal  $UO_2$ , cut and polished on a (111) plane. The substrate and source materials were placed in a silica tube approximately 6" apart. The silica tube was evacuated to  $10^{-7}$  mm pressure, refilled with the desired pressure of chlorine, sealed off and placed in a temperature gradient (about 25°C) furnace at an average temperature of 925°C. This results in transport of  $UO_2$  from the hot end to the cold end (i.e., onto the substrate).

The growth rate has been measured as a function of substrate temperature, temperature gradient and pressure of chlorine. The conditions for maximum growth, based on the thermodynamical calculations, give good quality single crystals. Characterization of the crystals by measuring

hardness, chemical composition, dislocation density and stoichiometry is continuing. X-ray and Debye-Scherrer patterns were taken in order to identify the structure and to determine the lattice parameter and stoichiometry. From five patterns taken (different samples) it was found that the crystals had fluorite structure and were a little hyperstoichiometric. An attempt was made to calculate the oxygen partial pressure generated due to the reaction of  $UO_2$  with chlorine by the following reaction:



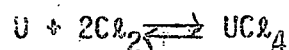
It was found that the equilibrium partial pressure of oxygen was enough to render  $UO_2$  crystals slightly hyperstoichiometric. For more accurate measurements, thermogravimetry is being used.

The microhardness measurements show a substantial decrease from an average value of 1050 for the substrate to a value of 450 for the crystals grown by CVD for a load of 50 gms. This suggests relatively higher purity and low dislocation density for the CVD grown crystals. To find the dislocation density a crystal was etched in a solution with 1 ml sulphuric acid, 7 ml water and 3 ml hydrogen peroxide. Optical microscopic examination showed two distinct kinds of etch pit shape that had developed. One has hexagonal or six fold symmetry while the other has three fold symmetry. The etching plane was (111) and dislocation etch pit should give three fold symmetry as is generally observed. One important point to note is that all the hexagonal etch pits developed at the site of triangular thermal etch pits developed during the growth of the crystal. In order to confirm whether the hexagonal etch pits correspond to dislocations, x-ray topography will be done. The above-mentioned observation as to the different shapes of etch pits is under further investigation. The dislocation density

perpendicular to the growth direction appears to decrease from a value of  $10^6/\text{cm}^2$  to  $10^4/\text{cm}^2$  as we go from the substrate to the crystal deposited by CVD. This also suggests a possibility of growing low dislocation density crystals. It is also hoped that the analysis of the data would shed some light on the kinetics of growth.

Although the closed system method of CVD growth of crystals is good for crystals of relatively small sizes, for larger crystals it is too time consuming. For larger crystals there are only two alternatives. First, grow for longer times, and secondly, to choose an open system for CVD growth. Looking at the growth rates, it was decided to go for open system because it is also planned to study the effect of thermal gradient on the O/U ratio and its relation to defect structure. This kind of study demands larger size crystals because of experimental limitations and also high purity crystals, so that impurities do not mask or complicate the effect of temperature gradient. Moreover, a flow system allows greater flexibility for control on the deposition and consequently the uniformity of the crystal.

For kinetic reasons it is decided to use temperatures as high as possible. We are building a furnace which can operate up to  $1800^\circ\text{C}$ . For initial runs chlorine would be used as carrier gas and uranium metal as a source material. The following reaction would be used:



uranium metal would be placed in an injector tube at a temperature high enough to render easy chloride formation ( $\text{UCl}_4$  in vapor phase). The

chloride is transported to the hot region, where a pre-established oxygen partial pressure would cause  $UO_2$  to deposit. The presence of a substrate at this site would make nucleation easier and the subsequent deposition would take place on the substrate. The stoichiometry of the crystal can be controlled by controlling the oxygen partial pressure in the system, i.e., by flowing  $H_2, O_2$  mixture or  $CO, CO_2$  mixture.

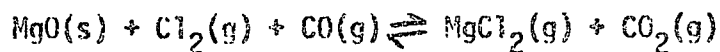
With the open system we will study the growth of  $UO_2$  single crystals as a function of total system pressure, flow rates of gaseous species, and temperature. An optimum growth condition would be found experimentally and thermodynamically. Once good quality crystals are available, we will study the effect of temperature gradients on chemical behavior and the dynamic dislocation behavior in  $UO_2$  single crystals.

## 2.2 Growth and Properties of CVD Grown Single Crystals of MgO and MgO- $Al_2O_3$

### Solid Solutions

(Professor W. D. Kingery, Professor H. K. Bowen; J. R. Booth)

The purpose of this research is to grow large, high purity single crystals of MgO and then to grow crystals of MgO doped with  $Al_2O_3$  in solid solution. The initial stage of the research involved surveying the thermodynamics of the possible reactions that would yield the desired crystals. It was desirable to have a reaction that had a free energy large enough to provide a positive driving force, yet not so large that it would be uncontrollable. Based on these restrictions, the following reactions were chosen:

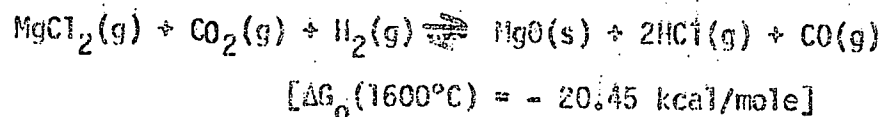


$$[\Delta G_0 (1000^\circ C) = - 30.5 \text{ kcal/mole}]$$

*see p. 51 bottom*

This was the basic reaction which formed the metal chloride. The large free energy of formation insures almost complete chlorination.

In the reaction chamber the reaction was reversed



Thus, by the addition of a single element the oxide was formed. By proper saturation and gas velocity the oxide formed as an epitaxial layer on substrates which were located within the reaction chamber.

The furnace was constructed with two concentric tubes. The inner tube was the injector which contains pellets of MgO. This tube ends in the center of the furnace. The outer tube was the reaction chamber which contains the substrates.  $\text{Cl}_2$  and CO flow through the injector and react with the MgO forming  $\text{MgCl}_2$  and  $\text{CO}_2$  which then leave the injector. Flowing around the outside of the injector is a mixture of  $\text{H}_2$  and argon. The argon was used for velocity adjustment around and from the injector to avoid turbulence.

The gas velocity was limited by three factors. The velocity must be laminar because turbulent flow causes nucleation in the gas phase and powder formation. Secondly, the velocity must be great enough to prevent back diffusion of  $\text{O}_2$  in the injector gas stream. Back diffusion results in formation of crystals on the injector nozzle. As these crystals grow they have a macroscopic effect on the gas flow pattern creating regions of turbulence. Thirdly, the velocity must not be so high that the gas goes through the reaction zone before it can react.

Crystals of MgO have been grown and are being analyzed. Initial observations indicate a very low dislocation density. Chemical analysis,



Berg-Barrett, Lang X-ray techniques and the electrical and optical measurements will all be conducted. These properties will be compared to existing "high-purity" commercial crystals.

### 2.3 Growth of Single Crystals of $ZrO_2-Y_2O_3$ Solid Solutions by Chemical Vapor Deposition in a Dynamic System

(Professor W. D. Kingery, Professor H. K. Bowen; L. P. Ferrao (supported partially by Fundacao de Amparo a Pesquisa do Estado de Sao Paulo))

Due to the failure in obtaining single crystals of  $ZrO_2-Y_2O_3$  solid solutions by chemical vapor deposition in a closed system, activity was shifted to the development of a dynamic system to accomplish the same purpose.

The system, as it is set up now, uses the reaction between a gaseous mixture of zirconium tetrachloride and yttrium chloride and carbon dioxide, under reduced pressure. The mixture of chlorides is generated inside the furnace by the reaction of chlorine gas with a yttrium-zirconium alloy of known composition, obtained by arc melting. Provided that this reaction takes place at a temperature high enough so that the vapor pressure of the resultant chlorides is larger than the system pressure, the Y/Zr ratio in the gas phase is the same as in the furnace.

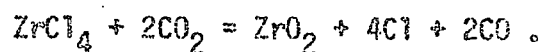
Initially, in order to permit greater flexibility in changing the ratio of yttrium and zirconium introduced in the furnace, generation of each chloride was made independently: zirconium chloride being generated externally by the reaction between zirconium metal and chlorine at 450°C (using argon as a carrier gas) and yttrium chloride being generated internally by a similar reaction at 1200°C. However, due to experimental difficulties, namely, clogging of the heated line connecting the  $ZrCl_4$  generator to the furnace (this line was necessary because  $ZrCl_4$  is a

solid at room temperature) and oxidation of Y metal inside the furnace due to small leaks of oxygen, this experimental approach had to be abandoned.

The experiments also pointed out the necessity of a careful design of the ejectors through which the gases are introduced in the furnace in order to avoid premature reactions and the possibility of clogging the various ejectors.

At this moment, it is possible to grow polycrystalline deposits of  $ZrO_2$ - $Y_2O_3$  solid solutions of controlled compositions under easily controlled and reproducible conditions. Attempts are being made to grow single crystals epitaxially on  $ZrO_2$ - $Y_2O_3$  single crystal substrates and at this point some of the experiments have been successful. The growth rate attained was 15-25 microns per hour. It is our aim at this moment to establish better conditions for the growth of single crystals improving both the quality and growth rate.

Parallel to the experiments described above, studies were undertaken to theoretically understand the thermodynamics and kinetics of the deposition process. In particular, a computer program was generated to determine the equilibrium conditions of the following reaction:



This is believed to be a good representation for the deposition process of  $ZrO_2$ , although approximate, because many other gaseous species can appear with lesser partial pressures. The development of a similar program for the deposition of  $Y_2O_3$  is under way. Also a more detailed study of the thermodynamics of the deposition process is being made.

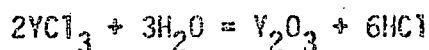
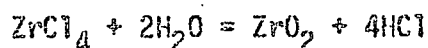
The results obtained from these studies up to this point enable us to evaluate the effects of the system pressure and the flow rates of the various gases on the supersaturation of the gas phase in

respect to depositing solids, therefore generating precious information on what must be done to improve the process.

#### 2.4 The Polycrystalline Growth of $Y_2O_3$ - $ZrO_2$ Solid Solutions by Chemical Transport

(Professor W. D. Kingery; C. C. Seaton)

The objective of this investigation was to establish conditions for the growth and control of vapor transported yttria-zirconia solid solutions. For deposition, the following reactions took place at 1400°C:



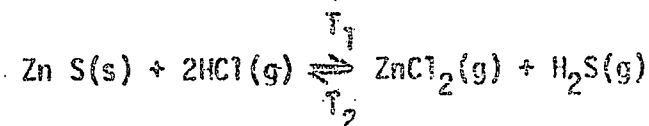
Zirconia can be deposited at a rate dependent upon the rate of gas flow. The rate of yttria deposition was limited by the method of chloride generation which prevented the co-deposition of yttria and zirconia, due to the large difference in deposition rates of both. Hence, the critical step in this research was the generation of yttrium chloride.

Procedures and equipment were developed for chemical transport. In order to achieve the above objective, further modifications are necessary (1) to find a method of yttrium chloride formation, the rate of which may be controlled by gas flows, and (2) to prevent the stoppage of flow by oxide deposition on the ejector tube.

#### 2.5 Chemical Vapor Deposition of ZnS on GaP

(Professor H. K. Bowen)

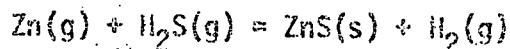
The deposition of ZnS on GaP has been studied in closed systems and in flowing systems. Previously, the results were reported for the flowing system involving the reaction:



Typical growth on 110 or 100 surfaces resulted in rates of 0.25 - 1 $\mu$ /hr.

Excess HCl led to etching and pitting of the substrates and therefore nonplanar junctions unless growth was restricted to low temperatures and low HCl concentrations.

To alleviate these problems a second reaction is being studied,



The zinc is introduced into the system by passing 2 cc/min Ar over liquid zinc at 820°C. The chemical potential of the sulfur in the gas phase that reacts with the Zn to form ZnS is controlled by the ratio of H<sub>2</sub>S/H<sub>2</sub>.

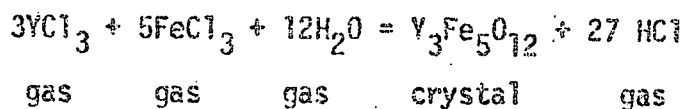
Excellent epitaxial growth was achieved by a ratio 2 cc/min H<sub>2</sub>S to 150 cc/min H<sub>2</sub>. A 3μ thick crystal was grown in 90 minutes on a 100 GaP substrate.

Experiments are continuing with the introduction of a dopant, Al, and with deposition occurring on 110 planes.

## 2.6 Growth of Single Crystal Epitaxial Films of Y<sub>3</sub>Fe<sub>5</sub>O<sub>12</sub> by Chemical Vapor Deposition

(Professor R. L. Coble; R. L. Gentilman\*)

Thin, epitaxial, single crystal films of Y<sub>3</sub>Fe<sub>5</sub>O<sub>12</sub> on nonmagnetic substrates have many potential magnetic device applications. The films are grown by chemical vapor deposition in a flowing system at 1200°C and 2 torr by the reaction:



To date, some single crystal films have been produced. The present research effort involves optimizing the crystal growth parameters in terms of crystal perfection. The growth of doped and gradient-doped films is planned for the future.

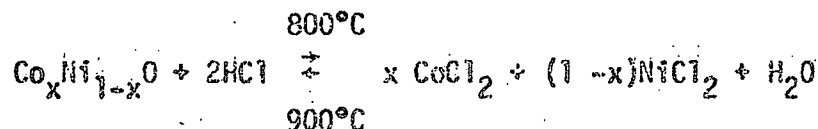
X no hard data

\*Not supported by this contract.

## 2.7 Chemical Vapor Transport and Phase Studies in $\text{Co}_x\text{Ni}_{1-x}\text{O}$

(Professor H. K. Bowen, Professor W. D. Kingery; M. Kinoshita)

Preparation of solid solutions of  $\text{Co}_x\text{Ni}_{1-x}\text{O}$  by chemical vapor deposition has been carried out well below the melting temperatures. Excellent control of homogeneity, stoichiometry and perfection was realizable when transport was in a closed system (evacuated quartz ampoules) and with HCl as the reacting transport gas. The deposition at 900°C yielded rates of 5-10 mg/hr. Composition control was maintained through the activity of the reacting powder constituents as given by:



A nearly linear relationship exists between the composition of the powder source and the single crystal deposit (some deviation in the data in the region  $\text{Co}_{.35}\text{Ni}_{.65}\text{O}$ ).

Crystal quality has been carried out by optical microscopy, X-ray and electron diffraction and transmission electron microscopy. Samples were thinned for TEM by ion bombardment thinning. Only isolated dislocations and no inclusions or voids were observable.

Annealing studies below 800°C have established the existence of a miscibility gap in the CoO-NiO system. Small single crystals were annealed in controlled oxygen atmospheres ( $\text{CO}_2/\text{CO}$ ) in order to prevent the formation of metal or of spinel. Transmission electron microscopy revealed a cubic second phase within the matrix with particle sizes from 200-800Å. The gap is asymmetrical and shifted to the cobalt rich side of the phase diagram.

? see  
p. 51  
from  
bottom?

*Co-doping in cooperation*

218 Co-Doping in Ultra-High Purity Materials

(Professor R. L. Coble; W. M. Smith)

Co-doping is the process of intentionally adding more than one impurity to a given material. Of particular interest are the effects of co-doping to maintain nominal electrical neutrality and avoid forming lattice defects. An example would be to add equal molar amounts of cation impurities with valence states one and three respectively to a material with a normal cation valence state of two. Presently, studies of the effects of adding small quantities of dopants are limited by the purity of the initial material. It is felt that studies made on materials of higher purity than is currently available would yield more significant results than can now be obtained. Therefore, an effort is being made to obtain materials of significantly higher purity than those now available on which to make studies.

At present a system is being designed utilizing an optically heated vertical floating zone to obtain desired purity. A vertical floating zone system was selected because it offers the advantages of crucibleless melting and atmospheric control. Crucibleless melting removes limits on the maximum temperature and eliminates contamination, both due to crucible material limitations. With atmospheric control selected impurities can be removed and recontamination prevented. Optical heating is limited only by the optical energy available and by the transmission spectrum of the sample being purified. The present design calls for Xenon-arc lamps as the source of optical energy. However provisions are being made for conversion to a laser source.

Tentatively fluorite,  $\text{CaF}_2$ , has been selected as the material on which initial studies will be made. Fluorite was chosen for early co-doping studies primarily because its structure is both relatively simple

and representative (thoria and urania having fluorite structure). While the optical coupling of fluorite is not good, it is felt that adequate power is available for purification. After purification the fluorite will be co-doped with single and trivalent cation impurities and the effects on properties noted.

In the future, the purification of many other materials to levels of ultra-high purity by a vertical floating zone system is contemplated. Various doping and co-doping experiments are planned. The studies made will not necessarily be very different from present studies. However, due to the improved purity of the new material, the future studies should be substantially more significant.

x no data

### 3.0 Electrical Properties

#### 3.1 Electrical Behavior of Amorphous Silicon as Revealed by Tunneling and Related Experiments

*see p.  
50, 4  
from top*

(Professor W. D. Kingery; J. Sauvage)

Tunneling into amorphous silicon through an oxide barrier was investigated at temperatures between liquid nitrogen temperature and room temperature. Tunneling was shown to be the preponderant conduction mechanism for the tunneling junctions used.

The tunneling junctions were sandwich configurations with a platinum bottom electrode, a layer of amorphous silicon, a silicon dioxide barrier and a platinum top electrode. They were evaporated and measured in a single vacuum cycle. Simultaneously a layer of amorphous silicon was deposited on coplanar contacts so as to correlate the tunneling and conductivity data.

Tunneling conductance was found to be temperature independent for tunneling into states of the semiconductor higher than the mobility edges. Tunneling into localized states of the semiconductor was found to depend exponentially on the third power of the inverse temperature. A simple model based on spatial localization of states within the mobility gap was developed to account for the observed temperature dependence. Using this model a density of states, at the Fermi level, of  $10^{20}$ /eV/cm was extracted from the tunneling data.

The mobility gap was found to be 0.8 eV, equal to the activation energy for electrical conduction at high temperatures. For low temperatures the conduction mechanism in amorphous silicon could be interpreted according to the Hopping model of Mott and the calculations of Halperin and others ( $T^{-1/4}$  dependence). The good agreement between the mobility gap, arrived



at from the tunneling measurements, and the activation energy for conduction in amorphous silicon at temperatures greater than about 500°K occurs by thermal activation of carriers from valence band-like extended states to conduction band-like extended states.

### 3.2 Effects of Thermal-Neutron Irradiation on Amorphous-Silicon Film

(Professor H. K. Bowen; L. P. C. Ferrao, D. D. Marchant, R. N. Singh, K. Uematsu)

Thin films (2700Å) of amorphous silicon were electron-beam evaporated onto fused silica substrates at  $10^{-7}$  Torr. Samples were then vacuum encapsulated in quartz ampoules and annealed at 300°C for 30 hours. They were subsequently subjected to integrated thermal-neutron fluxes up to  $8.3 \times 10^{18}$  n/cm<sup>2</sup>. Characterization of films before and after irradiation was accomplished by electrical resistivity, optical absorption, electron microscopy and EPR measurements.

The results indicate that carefully annealed samples of amorphous silicon are extremely resistant to thermal-neutron irradiation. As opposed to the resistivity changes of several orders of magnitude obtained when crystalline silicon is irradiated or similar variations induced in amorphous silicon upon annealing, only a factor of 4 decrease in resistivity occurs in amorphous silicon after a thermal-neutron flux of near  $10^{19}$  n/cm<sup>2</sup>. The optical absorption gap is essentially unchanged by irradiation. No structural changes as observed by transmission electron microscopy or electron diffraction were apparent. The resistivity and EPR (25% increase in free spins) results are consistent with the predominance of hopping conduction in the vicinity of the Fermi energy. The importance of these results is related to the eventual use of semiconductors in environments with extreme irradiation; for example, in nuclear reactor situations or solar cells which would have continued exposure from the Van Allen belt. Where crystalline

see  
p. 57,  
6 from  
bottom

silicon would have variable properties due to exposure, properly annealed amorphous silicon would have no changes.

Some studies are continuing to establish the effects of substrate temperature during deposition on the intrinsic optical and electrical properties. These results will be correlated with the past results from this laboratory of the dependence of the optical and electrical properties on annealing of silicon which was deposited at room temperature.

### 3.3 Electric Conduction Mechanism in Alumina

(Professor R. L. Coble; K. Kitazawa)

The mechanism of electric conduction in alumina is not established yet in spite of past extensive efforts because of uncertainties introduced by the presence of the external circuits on the sample surface or in the gas phase, or by the complexity of the electronic compensation method to eliminate the contributions from the external circuits. An attempt was made to thoroughly eliminate the above uncertainties by the use of specially shaped samples. The external paths were blocked by the sample wall itself, and hence no complex electrical circuits were introduced.

? see  
5 from  
bottom  
p. 57

The EMF of the electrochemical oxygen concentration cell and the conductivity measurement were carried out with the following results:

- (1) Both single and polycrystal alumina shows ionic conduction at low temperatures and become electronic conductive at high temperatures.
- (2) The transition temperature was around 1400-1500°C for the single crystal and 600-800°C for the MgO-doped polycrystal (LUCALOX) in air.
- (3) The transition temperature increases significantly with decreasing partial pressure of oxygen in the atmosphere.
- (4) The effect of this oxygen pressure takes place through the increase in the electronic contribution to the total conductivity, while the ionic contribution is essentially independent of the atmosphere.

(5) At a constant temperature, when the partial pressure of oxygen was decreased from one atmosphere, the total conductivity initially decreased until the pressure reached  $10^{-5} \sim 10^{-8}$  atmosphere. But it remained constant below this pressure range and hence did not show any conductivity minimum as reported earlier.

(6) Background conductivity measurements showed that the apparent conductivity increase at the lower oxygen pressure reported earlier with unguarded samples should be attributed to the increased gas phase conduction in the strongly reducing atmosphere.

As a conclusion, the present study has eliminated the uncertainties associated with the measurement methods to determine whether alumina is an ionic or electronic conductor. Generally, we can conclude that alumina is an electronic conductor at high temperatures or at high oxygen pressures and is otherwise ionic. The extent to which this transition is impurity dependent may be blamed for many of the variations reported in the literature.

#### 3.4 Stabilized Zirconia as an Oxygen Permeation Measurement Detector

(Professor R. L. Coble; K. Kitazawa)

Calcium-stabilized zirconia (CSZ) is now a well established oxygen ion conductor and can be used as an oxygen partial pressure detector as low as  $10^{-25} \sim 10^{-30}$  atmospheres. The application of CSZ to oxygen permeability of various oxides, therefore provides us with a highly sensitive, continuous and easy method of measurement. In order to make this application possible, the non-steady state behavior of CSZ after changing oxygen partial pressure must be fully understood.

In the present study a CSZ tubing was used both as the detector and as the sample through which the oxygen permeation rate was measured.

The change of oxygen partial pressure in the tubing was monitored by measuring the EMF on the porous platinum electrodes coated on both sides of the CSZ electrolyte. The following results were obtained: 1) The oxygen pressure in the tubing increases much slower than expected when the oxygen partial pressure is low in the tubing, which is probably due to the nonstoichiometry of CSZ electrolyte. Therefore, the apparent permeability under this condition is extremely small. 2) When the pressure in the system is more than  $10^{-4.5} \sim 10^{-3.5}$  atmosphere, the observed permeability agrees fairly well to the other available data taken under steady state conditions with a different method. 3) Using this pressure range the oxygen permeability was measured at different temperatures; the measurement was extended down to  $640^{\circ}\text{C}$  where the permeability was  $10^{-13}$  g/cm/sec (two orders of magnitude lower than the detection limit of the former measurement). 4) The mechanism of permeation in this region can be well explained by the ambipolar transport theory with electron holes as the rate-determining species. 5) The mobility and the concentration of the holes were calculated by the transient measurement. The mechanism of the hole conduction in CSZ was discussed; the results are consistent with holes being activated from deep acceptor levels, or acceptor level impurity band conduction. 6) The factors limiting the detection limit of the CSZ oxygen permeability detector is the nonstoichiometry of CSZ, the accuracy of the temperature control and the permeation through the CSZ detector itself. Considering those factors, CSZ can be applied to measure oxygen permeability with the detection limit  $10^{-13} \sim 10^{-14}$  g/cm/sec.

The oxygen permeability measurement of alumina with this method is in progress.

#### 4.0 Crystal Structure and Properties

##### 4.1 Nonstoichiometric Oxides with the Fluorite Structure Types

(Professor B. J. Wuensch; H. T. Anderson)

Many oxides of the type  $MO_2$  (where  $M$  is U, Th or a rare earth) display appreciable ranges of stoichiometry when  $O_2$  deficient. The defects involved appear to be vacancies in the oxygen array. There is direct evidence, as well as indirect evidence inferred from the properties of such materials, that the vacancies may order. In this study the nature of such ordering and the relaxation of the structure about a vacancy are to be determined through X-ray measurements.

The oxygen mobility in some of these nonstoichiometric oxides such as  $CeO_2$  is extremely rapid, even at room temperature. We therefore attempted to create vacancies by the addition of a trivalent ion, and thereby avoid potential problems involving compositional changes or gradients in specimens during study. A series of specimens ranging in composition from  $Ce_{0.9}Y_{0.1}O_{1.95}$  to  $Ce_{0.1}Y_{0.9}O_{1.55}$  have been prepared by ball-milling and pressing mixtures of the component oxides. The samples were equilibrated for periods up to one year at  $800^\circ C$ . No evidence of vacancy ordering was found. Wide ranges of solid solubility were observed, and a two-phase region (fluorite and rare earth type C) exists between  $Ce_{0.6}Y_{0.4}O_{1.8}$  and  $Ce_{0.3}Y_{0.7}O_{1.65}$ . In the single-phase region the lattice constants decrease as the structure changed from a disordered defect fluorite solid solution at low Y contents to a rare-earth type C structure. Similar variations of the lattice constants, but in systems with complete solid solubility, have been previously reported for samples equilibrated at  $1200^\circ C$ . We conclude that either no intermediate ordered phases occur in the system at this temperature, or that the kinetics of ordering are sufficiently slow so that the equilibrium structure is not attained.

We are presently examining the nonstoichiometric phases for  $\text{CeO}_{2-x}$ . The system had previously been studied with powder diffraction. Superstructures are difficult to define with such techniques, however, and we are accordingly using single-crystal specimens. Specimens of  $\text{CeO}_2$  are reduced in flowing hydrogen at a temperature selected to produce the desired composition, and then annealed in a  $10^{-6}$  Torr vacuum. The rapid oxidation rates require that the reduced sample be encapsulated in a sealed tube before removal from the vacuum. Techniques for accomplishing this have been perfected and the existence of the two phases with the greatest deviation from stoichiometry ( $\text{CeO}_{1.71}$  and  $\text{CeO}_{1.78}$ ) has been confirmed with powders. Also single crystal  $\text{CeO}_2$  was reduced to  $\text{CeO}_{1.71}$ , and the reciprocal lattice of the phase has been obtained. This information is currently being evaluated to produce the space group of this hexagonal phase. Twining has consistently been observed to occur during the formation of  $\text{CeO}_{1.71}$ .

#### 4.2 Strain Centers in Sapphire

(Professor R. L. Coble; C. V. Hari Rao)

The purpose of this study was to distinguish the contributions made by dislocations, impurities, and defects to the total microstrain present in crystals of sapphire. Methods employed were X-ray line breadth measurements and etch-pitting of dislocations.

Single crystals of alumina were grown by the various well known techniques, namely Czochralski, CVD, modified Bridgman and Vernueil. All the samples were oriented for the {0001} and {1120} planes, cut, polished, and annealed at  $1950^\circ\text{C}$  for 8 hours in a vacuum of  $10^{-5}$  mm. of Hg. Samples were cooled to room temperature slowly over a time period of 60 hours. The samples were quenched from various temperatures in the range of  $1550^\circ\text{C}$  to  $1950^\circ\text{C}$ , after holding for various times. During the annealing operations, two different atmospheres were used, namely, air and nitrogen, so that the defect concentrations can be controlled. X-ray line breadth measurements

were made of the  $\{11\bar{2}0\}$  reflections. The half-breadth was used as a measure of the total microstrain. Dislocation etch-pitting was accomplished by using Phosphoric Acid at  $320^{\circ}\text{C}$  as the etchant. This etches the  $\{0001\}$  face.

The dislocation density was quite constant; it did not change appreciably as a result of heat treatments. The half breadths, however, showed significant variation. However, it is hard to attribute all the strain to defects and impurities, and we suspect that the measured dislocation densities are low because the etch-pit technique is not very sensitive to detect small changes in dislocation density. The picture is more complicated by the fact that the impurities may exist in different valence states, thus changing the defect concentrations. More extensive testing is needed to clarify the picture.

*X no hard data*

#### 4.3 X-ray Topography of Oxides

(Professor R. L. Coble, Professor H. K. Bowen; J. L. Caslavsky)

A Berg-Barrett camera for the characterization of single crystals was set up and aligned. The primary function of the Berg-Barrett X-ray topographic facility was for the investigation of large crystals of MgO.

The direction of the Berger vectors in MgO are  $\langle 110 \rangle$ . Hence, to satisfy the extinction condition,  $\bar{g} \cdot \bar{b} = 0$ ,  $\bar{g}$  must have the directions given by  $\langle hh0 \rangle$ . From a consideration of the reflecting power of permissible planes, the  $\{220\}$  planes are most suitable for examination. However, the cleavage planes are  $\{200\}$  and the  $\{220\}$  planes are  $45^{\circ}$  from the cleaved surface. In order to obtain suitable diffracting conditions from these planes, using cleaved samples,  $\text{FeK}_{\beta}$  or  $\text{CrK}_{\alpha}$  X-radiation must be used.

Several samples of cleaved MgO were investigated under the above conditions and were characterized as follows.

The misorientation of mosaic blocks are between  $1^\circ$  and  $10^\circ$  with no preference to twist or tilt. The dislocation density is quite uniform and can be estimated at approximately  $10^6$ . The dislocations are highly decorated and can be characterized as being primarily tangles with a slight tendency to develop alignment.

The MgO crystals can also be characterized as possessing internal stresses most probably resulting from the temperature fluctuations during crystal growth. These stresses are easily relieved by annealing at  $600-650^\circ\text{C}$  resulting in the formation of slip bands parallel to  $\{220\}$  planes. The resulting slip bands are dominating features in the annealed crystals when investigated by X-ray topography and etching techniques.

#### 4.4 Dislocation Behavior in Pure and Doped (Fe) Single Crystals of MgO

(Professor R. L. Coble; R. N. Singh)

It has been observed that the presence of iron (Fe) in MgO increases the hardness and flow stress significantly. The level of increase depends not only on the doping level but also on the state of ionization and defect distribution created depending on the thermal history. Iron in trivalent state gives much more hardening and strengthening effect than iron in the divalent state. This is related to the dislocation interactions with the impurities which generate drag on them. However, the nature of the drag producing species is not yet known. The purpose of the present investigation is to determine the drag controlling mechanism for the dynamic dislocation behavior in crystals with Fe in trivalent and divalent states.

Experiments are in progress to determine the average dislocation velocity of edge and screw dislocations as a function of stress, temperature,



doping level and the state of ionization, by an etch pitting technique. Fresh dislocation loops are generated by an etch pitting technique. Fresh dislocation loops are generated by indenting the cleaved and chemically polished 100 surfaces. When stressed in a [100] direction (four point bending) these loops expand and the new dislocation loop position can be observed by re-etching the sample. Thus knowing the distance moved and the time of stress pulse one can determine dislocation velocity.

The results obtained at two impurity levels 24 ppm and 185 ppm Fe shows that the edge dislocations move faster than the screw dislocations, therefore, it is screw dislocation velocity which is rate determining step for the hardness and flow stress of these crystals. Moreover, the increase in the impurity level decreases the dislocation velocity by more than an order of magnitude. The stress exponent of dislocation velocity ' $m$ ' ( $v = A \tau^m$ ) seems to be temperature independent for 24 ppm Fe impurity for edge dislocations but slightly decreases with temperature for screw dislocations. However, at 185 ppm Fe impurity, stress exponent ' $m$ ' is significantly higher than the 24 ppm Fe impurity level and decreases significantly for both edge and screw dislocations. A value for ' $m$ ' of 2.8 for edge dislocations in the crystal with 24 ppm Fe is the lowest ever observed for rock-salt structure materials. The above behavior suggests different types of drag controlling mechanisms operative at low and high purity levels. The analysis of the data would hopefully elucidate the drag controlling mechanism. Similar analysis would be done on crystals with Fe in divalent state and this would elucidate the drag-controlling mechanism for solid-solution hardening.

In order to better understand the observation that some of the screw dislocations move faster than the edges in  $\text{CaF}_2$ , it is suggested that this may be related to dislocation structure near an indentation mark.

To clarify this point dislocation structure under an indentation mark will be investigated using X-ray topography and electron microscopy for samples in two stages, i.e., as indented and indented and stressed for  $\text{CaF}_2$  and  $\text{MgO}$ . This would also establish the nature of dislocation loops and their Burgers vector would be determined unambiguously.

#### 4.5 Grain Boundary Sliding in Oxide Ceramics

(Professor R. L. Coble; R. M. Cannon)

In oxide ceramics, grain boundary sliding is known to play an important role in the high temperature deformation, and also the high temperature fracture. The few studies reported to date on sliding of oxide, or other ceramic bicrystals indicate that yield effects, and other non-Newtonian behavior are common, and further, that strong orientation and impurity dependencies exist. As a result of the lack of understanding about the sliding mechanisms, the proper role of grain boundary sliding in polycrystalline deformation mechanisms is difficult to assess or treat analytically. The current view is that sliding, per se, is not the rate limiting step in those cases where the creep data show good agreement with the diffusional creep models. However, it is considered likely that the non-Newtonian behavior reported in ultra-fine grained oxides is related to non-Newtonian aspects of boundary sliding; this view is supported by increasingly frequent observations of grain boundary dislocations in deformed oxides. However, for this type of behavior, no explicit models have been developed to relate the boundary sliding and concurrent grain shape change; this is due in part to the limited understanding of the sliding mechanisms. Consequently, greater understanding of the sliding mechanisms and phenomenological dependence of sliding on stress, strain, strain-rate and temperature would contribute to further understanding of the deformation of polycrystalline oxides.

Studies of sliding of bicrystals of oxides, particularly  $Al_2O_3$  and  $MgO$ , are being undertaken to determine the dependence on mechanical variables, boundary misorientation, and temperature and to correlate these results with microstructural observations in order to clarify the sliding mechanisms.

*X no data*

#### 4.6 Optical and Electrical Properties of Single Crystal $Fe_xO$ - $MnO$ Solid Solutions

(Professor W. D. Kingery, Professor H. K. Bowen; C. A. Goodwin)

*see p. 51  
4 from bottom*

Although they are similar in their crystal, magnetic and electronic structures, the iron-group transition metal oxides exhibit a wide range of electrical and optical properties which has not as yet been explained by one consistent theory or model. For example, wustite ( $Fe_xO$ ) seems to conduct by a thermally activated hopping mechanism over most of the temperature range and has a room temperature conductivity of about  $50 \text{ ohm}^{-1} \text{ cm}^{-1}$ .  $MnO$ , however, appears to fit a semiconductor model with a conductivity as low as  $10^{-15} \text{ ohm}^{-1} \text{ cm}^{-1}$  at  $25^\circ\text{C}$ .

Another complicating factor is that many previous experimental results are suspect because the samples were polycrystalline, had undetermined nonstoichiometry due to improper quenching, and had possibly large amounts of impurities which would cause compensation in intentionally doped samples.

In an attempt to elucidate the real properties of these materials, single crystalline solid solutions in the  $Fe_xO$ - $MnO$  system have been prepared in high purity form by the closed-tube chemical vapor deposition technique, using  $MgO$  crystals as substrates and  $HCl$  as the transporting gas. Also, several compositions have been grown by the tri-arc Czochralski technique. The crystals obtained by both methods are being used to study the variation in electrical and optical properties of each end member versus the amount of

doping oxide and the change in lattice parameter. Visible, near IR, and far IR absorption spectra, and IR reflectivity are currently being measured and interpreted for changes in absorption edge, crystal-field peaks, structure arising from nonstoichiometry, and the reststrahlen spectra. Also UV reflectivity and conductivity measurements are being initiated. This set of measurements should provide a critical test of existing theoretical models.

#### 4.7 Low Temperature Conductivity and Reflectivity of CVD Wustite

(Professor H. K. Bowen; B. H. Auker)

*see top of p. 51*

Chemically vapor deposited single crystal wustite was characterized by the use of optical, X-ray and electron microscopy. IR reflectivity and low temperature conductivity measurements were then performed upon the samples.

Optical examination showed the crystals to have subgrains of  $1 \text{ mm}^2$  size and an etch pit density of  $10^6/\text{cm}^2$ . No inhomogeneities or indications of disproportionment into magnetite was observed under transmission electron microscope magnifications up to 41,000x. Electron diffraction patterns showed superlattice structures corresponding to 2.68 unit cells.

Conductivity measurements were made upon  $\text{Fe}_{0.91}\text{O}$  as determined by X-ray analysis from room temperature to 57°K ( $18 \text{ ohms}^{-1}\text{-cm}^{-1}$  to  $4.0 \times 10^{-5} \text{ ohm}^{-1}\text{-cm}^{-1}$ ) by the van der Pauw method with the use of a constant current source and voltmeter. Measurements were extended from 47°K to 21°K ( $4.6 \times 10^{-6} \text{ ohm}^{-1}\text{-cm}^{-1}$  to  $3.2 \times 10^{-10} \text{ ohm}^{-1}\text{-cm}^{-1}$ ) by use of a battery voltage source and picoammeter. Above 126°K log conductivity versus reciprocal temperature was linear with an activation energy of 0.063 eV. Below 126°K a transition occurred followed by linearity of log conductivity versus  $T^{-1/4}$  for six orders of magnitude to 25°K. From 25°K to 21°K, the curve showed some flattening. This behavior indicated a polaron hopping mechanism and possible impurity conduction.

IR reflectivity data was obtained for  $\text{Fe}_{0.93}\text{O}$  from 4000 to 200 wave numbers. No reflectivity peaks were observed at energies higher than Reststrahl spectrum. The Reststrahl spectrum showed a very broad peak with nominal wavelength at  $410 \text{ cm}^{-1}$ . A secondary peak was at  $200 \text{ cm}^{-1}$  and a sideband was observed at  $575 \text{ cm}^{-1}$ .

#### IV. FUTURE PROGRAM

Research efforts will be continued in areas of basic importance for understanding, controlling, and improving ceramic products and processes. These include: (1) kinetics of ceramic processes and microstructure development, (2) relationship of properties to crystal structure, glass structure, and microstructure, (3) structure and properties of crystalline and non-crystalline solids, and (4) materials preparation and characterization. In each of these areas we have made and expect to make substantial contributions. Studies which constitute a major part of our activity which will be continuing activities are already described in the previous section on the present status.

During the last year we have extended our activities relative to solid solutions and nonstoichiometry and boundary phenomena in oxides also related to fluorite structure systems of which  $UO_2$  is a major example. The program plans for the coming year will not have any appreciable effect on that emphasis.

Budget limitations make it not feasible to continue substantial effort related to films of noncrystalline material; this work will be decreased during the coming year. Also, because of the reduction in number of students we will essentially only continue with the above described continuing programs. The only increase in emphasis will be given to preparation of high purity crystals.

#### V. CAPITAL EQUIPMENT

For carrying out current and proposed research programs, it is necessary to augment our capital equipment in the following areas:

- (a) Controls, power supply, for high-purity materials preparation by melt growth
- (b) Iridium crucibles/susceptor
- (c) Dual injector CVD furnaces

## VI. SCIENTIFIC PERSONNEL

### 1. Senior Staff

Professor Kingery and Professor Coble will continue as principal investigators. In all cases, the research program is organized, planned, and carried out in close consultation with the principal investigators. Professor H. K. Bowen will continue working with some of the students with whom he worked during Professor Kingery's absence, i.e., Professors Wuensch and Bowen will continue as during the past year.

### 2. Participating Scientific Personnel

#### (a) Professors

	Time Devoted to Research	
	9/1/72-5/31/73	6/1/73-8/31/73
W. D. Kingery	50%	2 months at 100%
R. L. Coble	50%	2 months at 100%
B. J. Wuensch	25%	2 months at 50%
H. K. Bowen	25%	2 months at 50%

#### (b) Graduate Students and Research Staff

H. T. Anderson (leaving in August 1972)

B. H. Auker (left January 1972)

J. R. Booth (leaving July 1972)

R. M. Cannon

U. Chowdry

L. Ferrao (leaving September 1972)

C. Goodwin (leaving January 1973)

T. Hidaka

K. S. Kim (left June 1971)

K. Kinoshita (left September 1971)

Dr. K. Kitazawa (leaving January 1973)

D. D. Marchant  
 J. Neve  
 L. Radonjic (leaving January 1973)  
 C. V. H. Rao (left September 1971)  
 D. J. Reed  
 W. L. Robbins (left February 1972)  
 J. Sauvage (left September 1971)  
 R. N. Singh (leaving September 1972)  
 G. Wei

Other students to be appointed from September 1972 admissions to Graduate School.

3. Support by Other Federal Agencies Involving the Same Personnel

- (a) Professor Kingery - None.
- (b) Professor Coble - 5% Air Force
- (c) Professor Bowen - 25% Office of Coal Research and Air Force
- (d) Professor Wuensch - 50% N.S.F.

Technical Overlap - None.

VII. FUTURE PLANS FOR SUPPORT BY OTHER FEDERAL AGENCIES INVOLVING THE SAME PERSONNEL

We plan that all directly identified ceramic research and the entire research support of Professor Kingery continue to be provided by this contract and that no support of other agencies be solicited for him. Professor Coble receives a small amount of support from the Air Force in assistance to Professor Bowen's research.

*Pages 47 & 48 Removed - Proprietary Inf.*



## VIII. FINANCIAL STATUS

(a) It is anticipated that all currently available funds will be expended by August 31, 1972.

(b) Budget. This research has continued at essentially a constant dollar level for the last few years. The impact of inflation, increased graduate student stipends, and increased overhead rates made it imperative to decrease the number of graduate students to be supported.

At the present time we have three graduate students associated with the research who have independent fellowship or teaching assistantship support. We shall endeavor to increase that contribution.

PUBLICATIONS(a) Theses

- B. H. Auker, "Reflectivity and Low Temperature Conductivity of CVD Wustite," S.M. Thesis, Department of Metallurgy and Materials Science, M.I.T., January 1972.
- ✓ K. S. Kim, "Cation Self-Diffusion in ZnO," Sc.D. Thesis, Department of Metallurgy and Materials Science, M.I.T., August 1971.
- K. Kitazawa, "Electrical Properties and Defect Diffusion Study in Alumina and Calcia-Stabilized Zirconia," Sc.D. Thesis, Department of Metallurgy and Materials Science, M.I.T., January 1972.
- ✓ J. Sauvage, "Electrical Behavior of Amorphous Silicon as Revealed by Tunneling and Related Experiments," Ph.D. Thesis, Department of Metallurgy and Materials Science, M.I.T., August 1971.

(b) Papers published or presented at technical meetings

- A. Mocellin and W. D. Kingery, "Interpretation of Microstructure Changes during the Heat-Treatment of Sintered Alumina," submitted for publication, J. Amer. Ceram. Soc.
- A. Mocellin and W. D. Kingery, "Creep Deformation Controlled by Boundary Diffusion in MgO-Saturated Large Grain Size  $Al_2O_3$ ," J. Amer. Ceram. Soc., 54 (7), 339-341 (1971)
- R. L. Coble and M. C. Flemings, "On the Removal of Pores from Castings by Sintering," Met. Trans., 2 409-415 (1971)
- R. L. Coble and S. Prochazka, "On the Morphological Stability of Two-Phase Structures," J. Appl. Phys (in press)
- ✓ R. L. Coble and F. Yen, "On the Break-Up of Tubular Voids in  $Al_2O_3$  Crystals," submitted for publication
- ✓ R. L. Coble, S. C. Samanta and F. C. A. Yen, "Kinetics for the Intermediate Stage Sintering of Silver," Phys. Sintering (in press)
- J. Sauvage and C. J. Mogab, "Electron Tunneling into Amorphous Silicon," J. Noncryst. Solids (in press)
- J. Sauvage, C. J. Mogab and D. Adler, "Temperature-Dependent Tunneling into Amorphous Silicon," Phil. Mag. (in press)
- R. R. Shaw and D. R. Uhlmann, "Effect of Phase Separation on the Properties of Simple Glasses: II, Elastic Properties," J. Noncryst. Solids, 5, 237-263 (1971)

- R. M. Hakim and D. R. Uhlmann, "Electrical Conductivity of Alkali Silicate Glasses," *Phys. Chem. Glasses*, 12 (5), 132-138 (1971)
- D. R. Uhlmann and R. M. Hakim, "Derivation of Distribution Functions from Relaxation Data," *J. Phys. Chem. Solids*, 32, 2652-2655 (1971)
- B. J. Wuensch, "The Crystal Chemistry of Beryllium," Chapter 4A in *Handbook of Geochemistry*, Vol. II/3, Springer Verlag, New York (in press)
- R. J. Tiernan and B. J. Wuensch, "Diffusion of  $Tl^+$  in Single-Crystal  $KCl$ ," *J. Chem. Phys.* 55, 4996-4999 (1971)
- R. J. Tiernan, "Calculation of Grain-Boundary Diffusion Parameters and Comparison with Experiment," *J. Appl. Phys.* 42, 5596-5600 (1971)
- R. J. Tiernan and B. J. Wuensch, "Grain Boundary Diffusion of Thallium in Potassium Chloride," (submitted to *J. Am. Ceram. Soc.*)
- K. S. Kim and B. J. Wuensch, "Cation Self-diffusion in Zinc Oxide. I. Lattice Diffusion," (submitted to *J. Am. Ceram. Soc.*)
- K. S. Kim and B. J. Wuensch, "Cation Self-diffusion in Zinc Oxide. II. Dislocation Pipe and Grain Boundary Diffusion," (submitted to *J. Am. Ceram. Soc.*)
- P. N. Dangel and B. J. Wuensch, "Growth of Zinc Sulfide by Iodine Transport," (submitted to *J. Crystal Growth*)
- H. K. Bowen, W. D. Kingery, M. Kinoshita, and C. A. Goodwin, "Chemical Vapor Deposition of Transition Metal Oxide Solid Solutions," *J. of Cryst. Growth* (in press)
- ✓ D. Adler, H. K. Bowen, L. P. C. Ferrao, D. D. Marchant and R. N. Singh, "Effects of Thermal Neutron Irradiation on Amorphous Silicon Films," *J. Noncryst. Solids* (in press)
- ? K. Kitazawa and R. L. Coble, "Ionic and Electronic Conduction in Single and Polycrystal  $Al_2O_3$ ," presented at the 74th Annual Meeting of the American Ceramic Society, May 6-11, 1972, Washington, D. C.
- ✓ C. A. Goodwin and H. K. Bowen, "Optical Properties of Single Crystal  $Fe_0-MnO$  Solid Solutions," presented at the 74th Annual Meeting of the American Ceramic Society, May 6-11, 1972, Washington, D. C.
- ✓ J. R. Booth, H. K. Bowen, and W. D. Kingery, "Growth and Properties of CVD Grown Single Crystals of  $MgO$ ," presented at the 74th Annual Meeting of the American Ceramic Society, May 6-11, 1972, Washington, D. C.
- R. L. Coble, "Diffusion Models for Initial Sintering: Effect of Particle Size Distribution," presented at the 74th Annual Meeting of the American Ceramic Society, May 6-11, 1972, Washington, D. C.
- ✓ K. Kitazawa and R. L. Coble, "Defect Diffusion Coefficient Measurement in Polycrystal  $Al_2O_3$ ," presented at the 74th Annual Meeting of the American Ceramic Society, May 6-11, 1972, Washington D. C.

? see  
p. 27